IL NUOVO CIMENTO VOL. 13 D, N. 7 Luglio 1991

Three-Half Harmonic Generation in Laser-Plasma Interaction: Evidence for Plasmon Propagation.

D. GIULIETTI (*), V. BIANCALANA, D. BATANI (**), A. GIULIETTI
L. GIZZI (***), L. NOCERA and E. SCHIFANO (*_*)
Istituto di Fisica Atomica e Molecolare - via del Giardino, 7-56100 Pisa, Italia

(ricevuto il 20 Settembre 1990)

Summary. — Side emitted $3\omega/2$ radiation was studied by interacting 1.064 μm laser light with plasmas obtained from exploding thin foils. Both focusing ($f/8$) and collecting ($f/7$) optics were designed in order to reduce the instrumental bandwidth of the $3\omega/2$ spectrum. Time-resolved spectra and time-resolved images were obtained and analysed. All the observed spectral features, including the substantial lack of a «blue» component, the amount of red shift and bandwidth, are consistent with the Karttunen theory of half-integer harmonics generated in plasmas. This theory takes into account the propagation of $\omega/2$ plasmons produced by «two plasmon decay» and their coupling with laser light.

PACS 52.50.Jm – Plasma production and heating by laser beams.
PACS 52.35 – Waves, oscillations and instabilities in plasma.

1. – Introduction.

The plasma region at density close to one quarter of the critical density n_c is of primary importance in laser-plasma interactions. Indeed, the laser frequency being close to twice the local plasma frequency, pairs of Langmuir waves can be resonantly excited. A consequence is the acceleration of electrons to suprathermal velocities. Moreover, Langmuir waves can couple with themselves or with laser light and produce emission of half-integer harmonics [1, 2].

In laser fusion experiments radiation at half-integer harmonics is the principal diagnostics of plasma conditions at $n_c/4$ [3, 4]. Particularly time-resolved images of the plasma at three-half harmonic allow to follow the motion of the quarter critical

(*) Also at Dipartimento di Fisica, Università di Pisa, Italia.
(**) Presently at ICF group, Dipartimento di Fisica, Università Statale di Milano, Italia.
(***) Presently at Blackett Laboratory, Imperial College, London, UK.
(*_*) Presently at LULI, Ecole Polytechnique, Palaiseau, France.

region [5-7]; on the other hand, time-resolved spectra can give information on the physics of electron waves [8-12] and, in principle, they allow a measurement of the electron temperature in the same region.

Extended experimental investigations [13-19] of $3\omega/2$ emission have been made, even if comparison with the theory was not always satisfactory. The $3\omega/2$ line is generally found to be shifted from the unperturbed $3\omega_0/2$ value (ω_0 is the laser light pulsation) and considerably broadened. Both red and blue shifts were observed, but the blue component was usually weaker and sometime absent. From the phase-matching conditions [1, 20-23] the $3\omega/2$ spectrum is found to depend on the direction of observation with respect to wavevector of the laser light. In a large number of experiments the focusing angle and/or the detection angle were considerably large [4, 8-11, 14, 17, 18]. This fact introduced a considerable instrumental broadening of the $3\omega/2$ line and made the spectral analysis in terms of physics of harmonic generation more difficult.

To reduce this source of uncertainty in the analysis of the $3\omega/2$ spectra, we performed the experiment with the aperture of the focusing and detection optics much smaller than in most of previous experiments; in these conditions the contribution of optics to the spectral broadening resulted much lower than the observed bandwidth, as shown below.

Thin plastic foil targets were used which burned through during the laser pulse. A self-similar model [24] provided us with a rough estimate of electron temperature and density scale length at the burn-through time.

The study of $3\omega/2$ radiation at 90° to the laser beam axis has been performed from time-resolved spectra and time-resolved images. Their analysis allowed us to evidence the refraction of plasmons created by two-plasmon decay (TPD) due to their propagation through the plasma density gradients. In fact, refraction, changing the $\boldsymbol{k}$-vector of the plasmon, makes it possible that plasmons created with different k's (and consequently different ω's) in a wide range could match with laser photons and produce a broad $3\omega/2$ spectrum at the given angle of detection.

In sect. 2 we summarize the theory of $3\omega/2$ emission, and specialize it to our experimental conditions. The experimental apparatus is presented in sect. 3. In sect. 4 and 5 the experimental results are reported and discussed.

2. – Three-half harmonic generation.

Possible mechanisms of $3\omega/2$ generation include plasma waves with frequency near to $\omega_0/2$, produced close to $n_c/4$ by TPD [25-27] and stimulated Raman scattering [28] (SRS).

In principle 3/2 harmonic of laser light can originate from both the coupling of the incident laser radiation with $\omega/2$ plasma waves or the coalescence of three of those waves. However, as the three-wave process is of higher order, coupling of laser radiation with the plasma wave is expected to prevail in our experiment. Thus only the latter process will be considered. Also we shall consider only TPD as the mechanism responsible for plasmon generation, due to its lower threshold as compared with SRS. Notice that our experiment was performed at nominal intensities which were considerably lower than most of other $3\omega/2$ experiments.

Let us now consider the spectral analysis of three-half harmonics. In this respect

one of the most interesting theoretical works has been done by Karttunen [1], to which we substantially refer in the following calculations. In TPD the pair of plasma waves satisfies the energy and momentum conditions:

$$\omega_0 = \omega_B + \omega_R \,, \qquad \boldsymbol{k}_0 = \boldsymbol{k}_B + \boldsymbol{k}_R \,, \tag{1}$$

with the dispersion relations for photons and plasmons

$$\omega_0^2 = \omega_p^2 + k_0^2 c^2 \,, \qquad \omega_{B,R}^2 = \omega_p^2 + 3k_{B,R}^2 v_e^2 \,, \tag{2}$$

where v_e is the electron thermal velocity, ω_B and ω_R are the plasmon frequencies, $\boldsymbol{k}_B$ and $\boldsymbol{k}_R$ their wavevectors and ω_p the local plasma frequency. In the limit of weak Landau damping of electron waves, *i.e.* $k_{B,R}^2 \lambda_D^2 < 0.1$, λ_D being the Debye length, (1) and (2) give

$$\omega_p \approx (\omega_0/2)\left(1 - \frac{3}{4}(k_B^2 + k_B^2)\lambda_D^2\right) \tag{3}$$

from which we obtain for the electron density n

$$n/n_c \approx (1/4)\left(1 - \frac{3}{2}(k_B^2 + k_R^2)\lambda_D^2\right).$$

The minimum electron density for TPD is determined by the Landau damping ($k_{B,R}^2 \lambda_D^2 \approx 0.1$), whereas the maximum density is given by the minimum value for ($k_B^2 + k_R^2$) which is roughly k_0^2. Consequently the density range for TPD to occur is defined by

$$(n/n_c)_{min} \approx 0.19 \,, \qquad (n/n_c)_{max} \approx (1/4)(1 - 3/2\, k_0^2 \lambda_D^2) \,.$$

The plasmon frequency spectrum is obtained from eqs. (2) and (3):

$$\omega_B \approx (\omega_0/2)(1 + (3/4)(k_B^2 - k_R^2)\lambda_D^2) \,, \qquad \omega_R \approx (\omega_0/2)(1 - (3/4)(k_B^2 - k_R^2)\lambda_D^2) \,.$$

With $k_B > k_R$ the plasmons (ω_B, $\boldsymbol{k}_B$), travelling with a wavevector component in the direction of the pump wave (*i.e.* having $\boldsymbol{k}_0 \cdot \boldsymbol{k}_B > 0$) are blue shifted, while the plasmons (ω_R . $\boldsymbol{k}_R$), for which $\boldsymbol{k}_0 \cdot \boldsymbol{k}_R$ can be either positive or negative (see fig. 1), are red shifted from the exact $\omega_0/2$ frequency. In the following we will call them «blue» and «red» plasmons, respectively.

In order to describe the 3/2 harmonic spectrum let us now consider the coupling between the laser e.m. wave and one of the electron waves (plasmons) generated by TPD. Firstly we discuss the most general case in which plasmons from TPD propagate through the plasma gradient before they couple with the pump photons [1]. Secondly we specialize to the case of coupling without any plasmon propagation.

In the first case the matching conditions for the $3\omega/2$ emission process can considerably change in space because in the quater critical region the $\boldsymbol{k}_{R,B}$ wavevectors dramatically depend on density. On the contrary $\boldsymbol{k}_0$ and $\boldsymbol{k}_{3/2}$ depend weakly on it. The wave propagation through a density gradient will change the $\boldsymbol{k}$ vectors in both absolute value and direction. If we just consider the absolute values

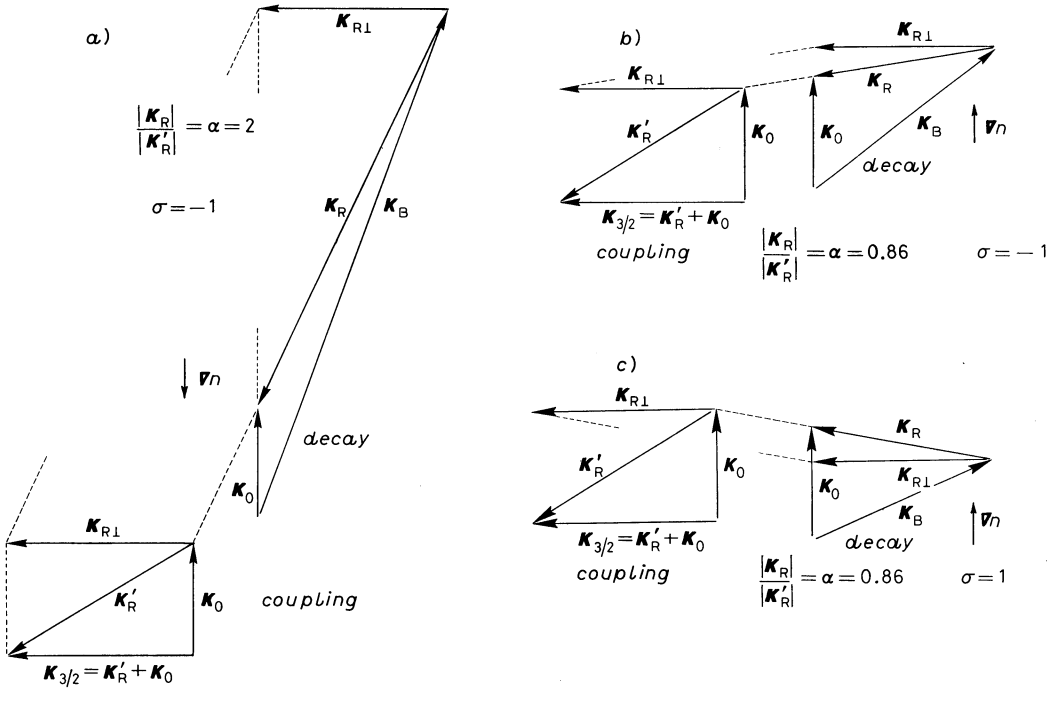

Fig. 1. – Generation of $3\omega/2$ at 90° to the laser beam direction. $\boldsymbol{k}$ vector composition of two-plasmon decay of laser light and coupling of laser photon with red plasmon $\boldsymbol{k}'_R$ after propagation: *a*) towards higher densities ($\alpha > 1$); *b*) and *c*) towards lower densities ($\alpha < 1$). The parameter $\sigma = (\boldsymbol{k}_0 \cdot \boldsymbol{k}_R)/|\boldsymbol{k}_0 \cdot \boldsymbol{k}_R|$ takes different signs in the three examples.

we can easily evaluate their change in terms of density variation:

$$\Delta k_0/k_0 = -[(\Delta n/2n)/(\omega_0^2/\omega_p^2 - 1)]_{n_c/4} = -(1/6)\,\Delta n/n\,,$$

$$\Delta k_{3/2}/k_{3/2} = -[(\Delta n/2n)/(\omega_{3/2}^2/\omega_p^2 - 1)]_{n_c/4} = -(1/16)\,\Delta n/n\,,$$

$$\Delta k_{B,R}/k_{B,R} = -(\Delta n/2n)/(\omega_{B,R}^2/\omega_p^2 - 1) = -(6k_{B,R}^2\lambda_D^2)^{-1}\,\Delta n/n\,.$$

Recalling that it must be $k_{B,R}^2\lambda_D^2 < 0.1$, we find

$$|\Delta k_{B,R}/k_{B,R}| > 1.7\,\Delta n/n\,,$$

which is much higher than both $\Delta k_0/k_0$ and $\Delta k_{3/2}/k_{3/2}$.

For laser radiation propagation along the density gradient (which is typical for exploding foils irradiated at normal incidence) and coupling with red plasmons as sketched in fig. 1, the energy and momentum conservation equations of the process

$$\omega_{3/2} = \omega_0 + \omega_R\,, \qquad \boldsymbol{k}_0 = \boldsymbol{k}_B + \boldsymbol{k}_R\,, \qquad \boldsymbol{k}_{3/2} = \boldsymbol{k}_0 + \boldsymbol{k}'_R$$

take the form

$$\omega_{3/2} = \omega_0 + \omega_R = 3\omega_0/2 - (3\omega_0/8)(k_B^2 - k_R^2)\lambda_D^2 , \tag{4}$$

$$k_B^2 = k_0^2 + k_R^2 - 2\sigma k_0 (k_R^2 - (k_{3/2} \sin\Theta)^2)^{1/2} , \tag{5}$$

$$k_R'^2 = (k_R/\alpha)^2 = k_{3/2}^2 + k_0^2 - 2k_{3/2} k_0 \cos\Theta . \tag{6}$$

In the derivation of eqs. (5) and (6) we assumed that the plasmon wavevector component perpendicular to the density gradient remains constant. Moreover, $k_0 = 3^{1/2}\omega_0/2c$ and $k_{3/2} = 2^{1/2}\omega_0/c$ are the wavevectors for ω_0 and $3\omega_0/2$ radiation at $n_c/4$, Θ the angle between them, $\sigma = (\boldsymbol{k}_0 \cdot \boldsymbol{k}_R)/|\boldsymbol{k}_0 \cdot \boldsymbol{k}_R|$ and α the ratio of the modulus k of the plasmon produced by TPD and the modulus k' of the same plasmon after the propagation.

From eqs. (4)-(6) we obtain, for the emitted three-half harmonics

$$(\omega_{3/2} - 3\omega_0/2)/\omega_0 = -(3/8)(k_0 \lambda_D)^2 [1 - (2\sigma/3^{1/2})(11\alpha^2 \pm 4 \cdot 6^{1/2}\alpha^2 \cos\Theta - 8\sin^2\Theta)^{1/2}] ,$$

from which we find the wavelength shift from the exact $2\lambda_0/3$ value

$$\Delta\lambda_{3/2} = (\lambda_0/2)(v_e/c)^2 [1 - (2\sigma/3^{1/2})(11\alpha^2 \pm 4 \cdot 6^{1/2}\alpha^2 \cos\Theta - 8\sin^2\Theta)^{1/2}] . \tag{7}$$

Notice that the «−» sign refers to the incident photon $(\omega_0, \boldsymbol{k}_0)$ and the «+» sign to the reflected one $(\omega_0, -\boldsymbol{k}_0)$ which may be present (*e.g.* due to Brillouin backscattering or critical layer reflection).

In fig. 1 the vector composition is graphically shown for two-plasmon decay and coupling after propagation of the red plasmons in three different cases. In fig. 1*a*) the red plasmon has a component opposite to the photon wavevector ($\sigma = -1$) and it propagates towards higher densities into the plasma (we choose $\alpha = 2$). In fig. 1*b*) and *c*) the red plasmon propagates towards lower densities and is characterized by $\sigma = -1$ and $\sigma = 1$, respectively.

Commutating the indices B and R in eqs. (4) to (6) and in σ, the equivalent shift in the case of coupling with blue plasmons is obtained. The expression will be formally the same as (7). However, while in the case of red plasmons σ can assume both the values ± 1, in the case of blue plasmons only $\sigma = 1$ is allowed.

As is evident from (7) the plasmon propagation results in an additional shift of $3\omega/2$ radiation, the ordinary shift being an effect of the plasma temperature. Because an α-range is possible (as discussed below) the plasmon propagation is a source of $3\omega/2$ line broadening as well.

At $\Theta = 90°$, as in our experiment, (7) simply reduces to

$$\Delta\lambda_{3/2} = (\lambda_0/2)(v_e/c)^2 [1 - (2\sigma/3^{1/2})(11\alpha^2 - 8)^{1/2}] . \tag{8}$$

In the simpler case in which plasmons couple with pump photons ω_0 to generate $3\omega/2$ in the same place where they are produced by TPD ($\alpha = 1$), the wavevector composition for the two processes is like the one shown in fig. 2. This figure evidences that $3\omega/2$ can be emitted at 90° from the laser beam direction in two ways. In the first pump photons couple with backpropagating red plasmons. This is a «direct» emission,

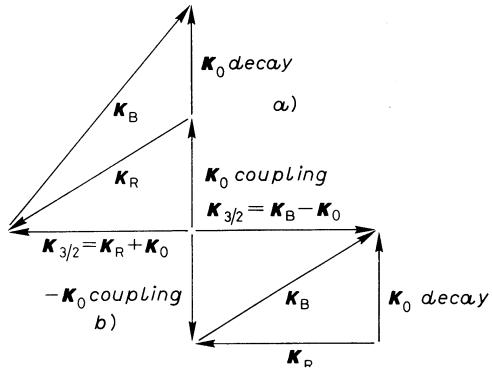

Fig. 2. – Generation of $3\omega/2$ at 90° to the laser beam direction. Coupling of a pump (*a*)) or backpropagating (*b*)) photon with a TPD plasmon, in the some place where it is produced.

because neither the photon nor the plasmon suffer reflection before coupling to generate $3\omega/2$. In the second way reflected photons interact with blue plasmons generated by TPD of impinging laser photons. This is an «indirect» emission. In this case $\boldsymbol{k}_{3/2} = -\boldsymbol{k}_R$, regardless of the value of the angle Θ.

It is important to notice that $3\omega/2$ spectra can give a measurement of electron temperature in the $n_c/4$ region if the spectral component related to $\alpha = 1$ is identified. This is not generally possible due to the the fact that a wide range of k's values are possible for plasmas, so that a range of values may be assumed by the parameter α. However, in some conditions the temperature can be estimated from the red or blue limit of the spectrum when they are attributable to Landau damping. This point will be further discussed in sect. 5 (see also fig. 5).

3. – Experimental apparatus.

A Nd laser ($\lambda_0 = 1.064\,\mu$m, spectral width $\Delta\lambda \approx 0.7$ Å) delivering an energy E_L up to 3 J in $\tau_L = 3$ ns (FWHM), was focused on target by an $f/8$ lens into a vacuum chamber. In a 60 μm diameter focal spot a nominal intensity up to $5 \cdot 10^{13}$ W/cm^2 was reached.

Prepulse level was maintained below 10^{-4} times the main pulse except for a small number of shots. Time modulations were present into the pulse, due to beating of longitudinal modes in the laser cavity.

Here and in the following we refer to a «nominal intensity» simply calculated as $E_L/\tau_L S_L$, where S_L is the spot area. This is only a reference parameter. The actual intensity reached higher values temporally, due to the pulse modulation and, spacially, due to the intensity distribution of the laser beam. A further increase was possibly due to self-focusing.

The targets we used consisted of thin formvar foils (polyvinyl formal $[C_5H_{11}O_2]$; density = 1.1 g/cm^3; $Z_a = \langle Z^2 \rangle / \langle Z \rangle \approx 3$, where Z is the ion charge and $\langle\ \rangle$ denotes an average over all the ions), whose thickness, ranging from 0.1 μm to 1.6 μm, was measured with an interferometric method [29].

The target was irradiated at normal incidence to its surface and the laser light was linearly polarized at 45° with respect to the detection axis. At nominal intensities above 10^{13} W/cm^2 and foil thickness up to 1.5 μm the targets were definitely burnt through during the laser pulse, as observed with transmission measurements. We did not measure the burn-through time, but the 1D model [24] supplied us with an approximate upper limit, being the plasma expansion partially 2D at the peak of the pulse.

The radiation was collected at 90° from the beam axis, using an $f/7$ optics, and imaged into the entrance slit of a spectrometer coupled with a Hadland streak camera. The overall spectral resolution resulted 3 Å and the time resolution was 20 ps. The collecting optics was designed in order to have no spatial selection of the $3\omega/2$ source. Spectral calibration was performed with the 7032 Å, 7174 Å, 7245 Å lines of Ne. A wavelength fiducial was obtained putting a thin wire on the spectrometer output plane, perpendicularly to the dispersion axis. The position of the wire was in turn calibrated with the same spectral lines.

Alternatively, to obtain the time-resolved images of the emitting regions, the interaction region was imaged directly into the entrance slit of the streak-camera with a magnification $G \approx 10$. $3\omega/2$ light was selected by a narrow-band interference filter, 100 Å FWHM band-pass, centred at 7090 Å. The streak-camera slit was superimposed to the laser beam axis in the image of the plasma. The slit aperture was set in order to match the focal spot diameter and the spot image was carefully positioned. This set-up allowed to locate the position of the $3\omega/2$ source (*i.e.* the $n_c/4$ layer) along the interaction region.

4. – Experimental results.

The aim of the experiment was the study of the spectrum of $3\omega/2$ radiation. We also measured the nominal intensity threshold for such an emisssion, which resulted $I_{thr} \approx 5 \cdot 10^{12}$ W/cm^2. Another observation was that $3\omega/2$ emission completely disappeared in case of a prepulse level higher than 10^{-4} the main pulse. This is due to the fact that, in such a condition, the plasma is produced earlier and the electron density is lower than $n_c/4$ at the time of the main pulse.

In fig. 3 and fig. 4 some time-resolved spectra and time-resolved images are reported. A time modulation in a time scale of tens of picoseconds is apparent. It is due to the intensity modulation already present in the laser pulse. However, we observed that such modulations resulted strongly enhanced in scattered $3\omega/2$ radiation: actually $3\omega/2$ intensity depends at least quadratically on the impinging laser intensity [2, 30].

Figure 3 shows two typical time-resolved spectra as observed with targets of 1.0 to 1.5 μm thickness at nominal intensity 1 to $3 \cdot 10^{13}$ W/cm^2, respectively. The wavelength fiducial looks like an artificial intensity minimum at 7127 Å: it has to be ignored in the spectral analysis. The dashed line parallel to the time axis shows the position of the exact $3\omega_0/2$ line. $3\omega/2$ spectra showed a strong variability from one spike to another, either for what concerns shift and width. A general feature was that the spectra were red-shifted and only few spikes showed a faint blue component, too.

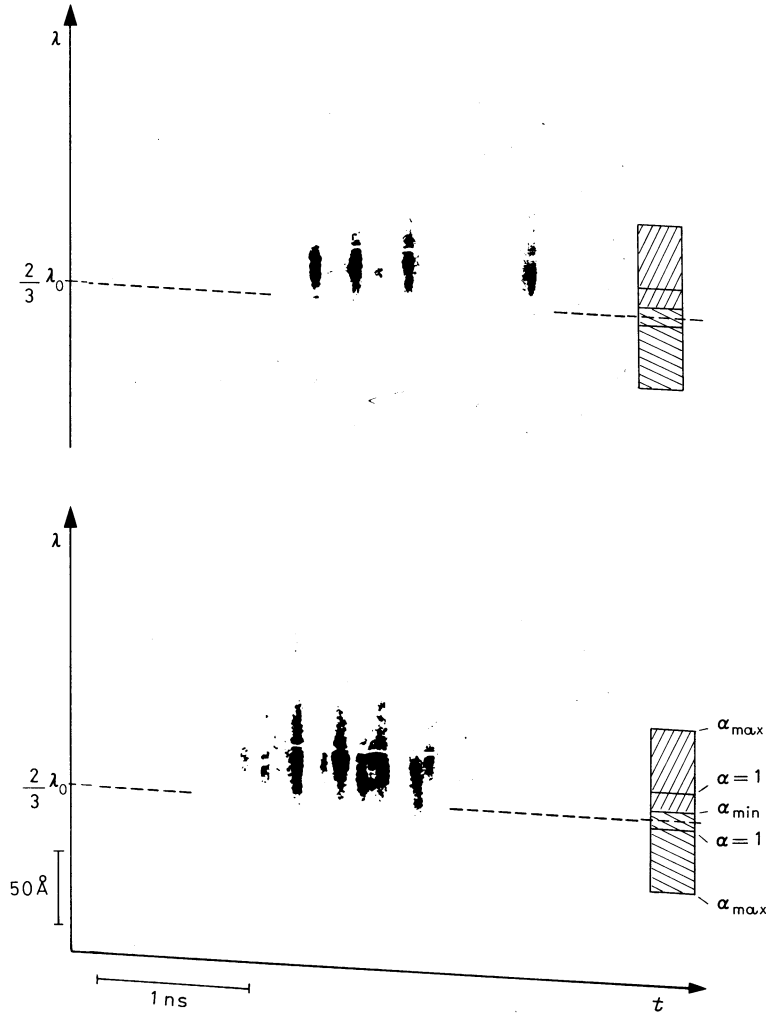

Fig. 3. – Two typical time-resolved spectra of 3/2 harmonic emitted perpendicularly to the beam axis. Lower image: shot No. 171206, formvar foil thickness $d = 1.50\,\mu$m; laser intensity on target $I = 1.4 \cdot 10^{13}$ W/cm^2. Upper image: shot No. 171207, $d = 1.50\,\mu$m, $I = 1.4 \cdot 10^{13}$ W/cm^2. Right-hand side of each spectrum, a box shows the characteristic values of the parameter α, as given by theory, calculated at $T_e = 0.6$ keV (see also fig. 5).

Often only the $\sigma = -1$ region of the spectrum was apparent. Both the red shift and spectral width were found to decrease when the laser peak power decreased.

Figure 4 shows two typical time-resolved images of the $3\omega/2$ emitting region. Notice that the emitting region is moving in time along the beam axis; this motion was also inferred from 2ω spectra obtained in the same experiment [31]. The $3\omega/2$ emitting region was also observed to split during the pulse duration. This fact evidences the motion of $n_c/4$ region along the density profile. From the images we

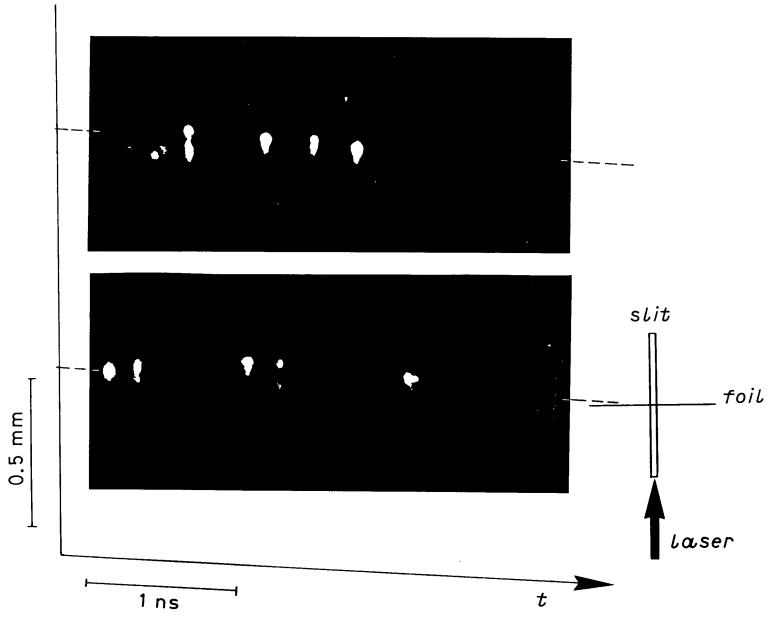

Fig. 4. – Two typical time-resolved images taken with a narrow band 7090 Å filter, showing the evolution of the 3/2 harmonic sources into the plasma. Lower image: shot No. 020215; $d = 1.43\,\mu m$, $I = 1.3 \cdot 10^{13}\,W/cm^2$. Upper image: shot No. 020203; $d = 0.80\,\mu m$; $I = 1.3 \cdot 10^{13}\,W/cm^2$.

can estimate the scale length of the density gradients in the $n_c/4$ region. We found values of a few tens of micrometers, which reasonably agree with the expansion model [24].

The evolution of $3\omega/2$ sources was not well reproducible shot by shot due to the spiking behaviour of the pulse. However, there was a general trend for each $3\omega/2$ burst as follows: the emission started from a single dot source, then the source splitted into two dots and finally recombined back in a single one.

It is interesting to observe that, while the $3\omega/2$ radiation was characterized by well-defined regions of emission and a broad spectrum, the 2ω radiation at 90° to the beam axis in the same experiment [31] was emitted from wide plasma regions with a narrow spectrum. This is an indication of completely different mechanisms of emission for the two cases. In fact, $3\omega/2$ radiation can be emitted only in a density region close to $n_c/4$ via the interaction of e.m. waves with plasmons of broad energy spectrum; on the other hand, 2ω radiation is generated at 90° by the interaction of two counterpropagating e.m. waves having about the same bandwith as the laser light; this process can take place virtually in the whole laser plasma interaction volume.

5. – Discussion.

First of all let us briefly discuss the $3\omega/2$ source structure and its evolution as depicted by the time-resolved images in fig. 4. The overall duration of the harmonic emission was typically 1 to 2 nanoseconds, depending mostly on laser intensity and

foil thickness, with some nonreproducibility due to the spiking intensity modulation in the pulse. As evidenced in the last section a single emitting layer is observable at the beginning, then splitting into two layers and finally merging again into a single source. This behaviour is consistent with an early $3\omega/2$ generation in the $n_c/4$ region ahead the critical front, towards the focusing lens, followed by the activation of another $n_c/4$ region beyond the density maximum after burn-through; then the two $n_c/4$ regions recombine at the top of the density profile just before the end of the emission. The delay between burn-through and the time when the maximum density is $n_c/4$ has been evaluated with a 1D model [24] in the conditions of the present experiment. It results of about 1ns, a value comparable with the mean delay we observed from the source splitting to the end of the emission. This is only a rough modelling of the harmonic source evolution; for a more precise analysis one should consider the partial 2D late expansion and the possible contribution of marginal regions of laser-target interaction, where near-critical plasma could be present.

The analysis of the spectra comes from the assumption that in our experimental conditions the emisssion is mostly due to the coupling of pump photons $(\omega_0, \boldsymbol{k}_0)$ with plasmons $(\omega_{B,R}, \boldsymbol{k}_{B,R})$ from TPD. The spectra of $3\omega/2$ light emitted at 90° we obtained are characterized by considerable values of both red shift and bandwidth. Such values are very difficult to explain if the propagation of TPD plasmons is not considered. Recall that in case of nonpropagating plasmons the shift is given by eq. (8) with $\alpha = 1$, $\sigma = -1$. The electron temperature was measured from the Brillouin red shift [31] to be $T_e \approx 0.6\,\mathrm{keV}$, in reasonable agreement with the theoretical model [24]. At this temperature, from eq. (8) with $\alpha = 1$, the expected shift is $\Delta\lambda_{3/2} \approx 19\,\text{Å}$.

Another possible source of shift is the Doppler effect due to plasma flow through the $n_c/4$ region, which is essentially parallel to the electromagnetic-wave propagation. If v is the flow velocity, the laser light is «seen» in that region as having a pulsation $\omega_0[1 \pm (v/c)]$. The further shift one gets inserting such pulsation into eq. (8) is $\Delta\lambda_d = \mp\lambda_0(2v/3c)$. The upper and lower signs refer to the $n_c/4$ regions ahead and behind the target respectively. Notice that no Doppler correction is due to the $3\omega/2$ light propagating 90° to the plasma flow. Assuming a near-sonic flow at the $n_c/4$ layers, the Doppler shift so calculated is $\Delta\lambda_d \approx \pm 5\,\text{Å}$. As a matter of fact both temperature and Doppler effects give shifts lower than the mean shift we observed on a large number of shots ($\approx 35\,\text{Å}$).

More pronounced is the discrepancy for the $3\omega/2$ bandwidth. In fact in case of nonpropagation we can take into account several causes of line broadening. First collisional broadening: the electron-ion collision frequency is related to the damping coefficient Γ_c of a plasma wave (of complex frequency ω) by the relation

$$\Gamma_c = \mathrm{Im}\,\omega = \nu_{ei}/2\,.$$

In our conditions (T_e in keV)

$$\nu_{ei} \approx 6.7 \cdot 10^{-11}(Z n_e \ln \Lambda T_e^{-3/2}) \approx 8 \cdot 10^{11}\ \mathrm{s}^{-1}\,,$$

so the collisional width $\delta\omega = 2\Gamma_c$ gives $\delta\lambda_c \approx 2.1\,\text{Å}$.

Second broadening due to Landau damping: it is negligible in our experimental conditions for $3\omega/2$ observed at 90° since $(K_{B,R}\lambda_D)^2 \approx 10^{-2}$.

Finally the effect comes of the aperture of focusing (θ_F) and collecting (θ_C) optics giving, from eq. (7) at $\Theta = 90°$, $\delta\lambda_{aper} \approx 1.5\lambda_0(v_e/c)^2(\theta_F + \theta_C) \approx 3.6\,\text{Å}$. Notice that in most of the previous experiments with planar targets much larger aperture focusing optics

were used, often close to $f/1$ [8, 9, 11, 14, 17, 18]. A variety of apertures were used in the detection optics in those experiments. Large aperture in focusing and/or detection optics results in an instrumental broadening of the $3\omega/2$ line. As an example we estimate that an $f/1$ optics can produce approximately a 30 Å bandwidth with a 0.6 keV plasma.

Due to the causes considered above, the $3\omega/2$ line can be broadened in our experiment just by a few Å, a small extent if compared with the observed bandwidth of several tens of Å. Thus the propagation of the electron waves before they couple with the e.m. wave has to be considered to explain both shift and broadening.

From the analysis of sect. 2 we know that the $3\omega/2$ radiation we detected at 90° is mostly a «direct» emission produced by coupling of the impinging laser radiation with red plasmons $(\omega_R, \boldsymbol{k}_R)$ having $\sigma = -1$. However, we will consider also the «indirect» emission which can be given by the coupling of $\omega/2$ plasmons reflected by the $n_c/4$ layer. In this case we denote with reflection a particular case of propagation which is able to invert the component of the plasmon momentum along $\boldsymbol{k}_0$. Another possibility of indirect emission is given by the interaction of plasmons with backpropagating laser photons; however both reflection and backscattering of laser light were very weak in this experiment.

Using eq. (8), in fig. 5 we reproduced a possible $3\omega/2$ spectrum allowed by plasmon propagation *vs.* electron temperature. The dash-dotted line corresponds to the exact $(2/3)\lambda_0$ value (7093 Å). First of all we observe that in eq. (8) α can assume two limiting values: $\alpha_{min} \approx 0.85$ (for $\alpha < \alpha_{min}$ the matching condition for wavevectors cannot be fulfilled), and

$$\alpha_{max} \approx k(\text{at minimum density})/k'(\text{at coupling density}) = [k^2/(k_0^2 + k_{3/2}^2)]^{1/2} \approx 2T_e^{-1/2} ,$$

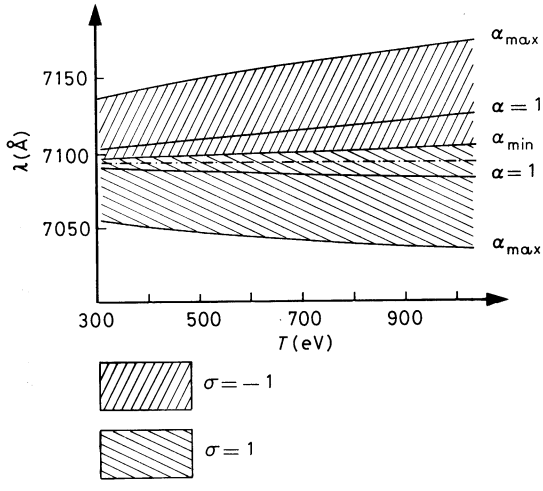

Fig. 5. – Spectrum *vs.* temperature for different values of the propagation parameter α and geometrical parameter σ. The dash-dotted line indicates the unperturbed 3/2 harmonic position: $2\lambda_0/3$. The spectral range between α_{min} and α_{max} corresponds to the maximum bandwidth of 3/2 harmonic emission in case of propagation of plasmons before coupling. Notice that taking into account only temperature effects (no propagation: $\alpha = 1$) the harmonic line is not located at the centre of the allowed band.

where k is determined by Landau damping, k' by the detection at 90° and T_e is in keV.

The two differently dashed regions in fig. 5 correspond to different directions of the plasmon wavevector component along $\boldsymbol{k}_0$ and are defined by the geometrical parameter σ.

The lines $\alpha = 1$ correspond to the position of blue and red components in the case of nonpropagating plasmons. Notice that the lines $\alpha = 1$ are not in the centre of the allowed spectral regions. For this reason an attempt to estimate electron temperature from the centre of the $3\omega/2$ band would lead to a considerable error. On the contrary, if the plasmon propagation is considered, the $3\omega/2$ spectra we observed are roughly consistent with the allowed α-range for $T_e = 0.6\,\mathrm{keV}$: this is the temperature which the boxes of fig. 3 refer to.

The blue component of the 3/2 harmonic was usually absent in our spectra or very weak in a few spikes. This is not surprising because the contribution of photons reflected at the critical layer or due to Brillouin backscattered is very weak as already mentioned. The lack of a significant blue component also means that the reflection of $\omega/2$ plasmons propagating in the $n_c/4$ region is not an efficient process.

Finally some considerations about the threshold. We observed a threshold for 3/2 harmonic emission at nominal laser intensity of $5 \cdot 10^{12}\ \mathrm{W/cm^2}$. Being $3\omega/2$ emission a secondary process, we expect that its threshold is higher or comparable with the TPD threshold. On the contrary the measured value of the nominal intensity threshold for $3\omega/2$ emission is much lower than the expected threshold for TPD. In fact, if we consider the theoretical thresholds I_{coll} and I_{inh} for exponential growth of the instability in the two cases of collision or inhomogeneity dominated process respectively [16, 24], we find in our experimental condition $I_{\mathrm{coll}} \ll I_{\mathrm{inh}}$. Using in I_{inh} an $n_c/4$ layer scale length of 30 μm, which is a mean value of measurements taken from time-resolved images, the TPD threshold can be estimated of the order of $10^{14}\ \mathrm{W/cm^2}$. This is only an apparent discrepancy because, as discussed in sect. 3, the maximum intensity reached during the interaction is certainly higher than the nominal intensity.

6. – Conclusions.

Irradiation of thin foil targets with a laser beam focused at large f/number and detection of scattered light with large f/number optics is very effective to take spectroscopic information on parametric processes where the matching between wave momenta critically depends on angles. We studied $3\omega/2$ emission in such experimental conditions.

With normal incidence irradiation of plastic foils $\approx 1\,\mu\mathrm{m}$ thick at laser intensities of the order of $10^{13}\ \mathrm{W/cm^2}$ we observed $3\omega/2$ emission perpendicularly to the laser beam. This emission showed a spiky character with spikes of tens of picoseconds. The harmonic generation was definitely missing in the presence of significant prepulse in the laser light. Time-resolved imaging in $3\omega/2$ light allowed a measurement of the $n_c/4$ layer scalelength. It was found to be typically a few tens of micrometers.

$3\omega/2$ data analysis gave information on two-plasmon decay process. Time-resolved spectra showed variability spike to spike in the same shot, but the mean values of shift and bandwidth were reasonably reproducible shot by shot. Mean values of red shift is about 35 Å and bandwidths were observed up to 100 Å; they cannot be explained

in terms of the theory of TPD-driven $3\omega/2$ emission, unlesss the propagation of $\omega/2$ plasmons into the plasma is considered. Including the latter process into the calculations, the observed spectral features were satisfactorily explained.

* * *

The continuous, creative technical assistance of S. Bartalini was essential to the experimental work. Authors are also indebted to Cyril Brown and the target preparation group of the Laser Division at Rutherford Appleton Laboratory for transferring of information on thin-target fabrication. Comments and suggestions from E. Fabre, C. Labaune and F. Amiranoff were precious to the data analysis. This work was fully supported by Consiglio Nazionale delle Ricerche, Italy.

REFERENCES

[1] S. J. KARTTUNEN: *Laser Part. Beams*, **3**, 157 (1985).
[2] R. L. BERGER and L. V. POWERS: *Phys. Fluids*, **28**, 2895 (1985).
[3] V. YU. BYCHENKOV, V. P. SILIN and V. T. TIKHONCHUK: *Sov. J. Plasma Phys.*, **3**, 730 (1977).
[4] W. SEKA, B. B. AFEYAN, R. BONI, L. M. GOLDMAN, R. W. SHORT, K. TANAKA and T. W. JOHNSTON: *Phys. Fluids*, **28**, 2570 (1985).
[5] S. JACKEL, B. PERRY and L. LUBIN: *Phys. Rev. Lett.*, **37**, 95 (1976).
[6] LIN ZUNQI, TAN WEIHAN, GU MIN, MEI GUANG, PAN CHENGMING, YU WENYAN and DENG XIMING: *Laser Part. Beams*, 4, 223 (1985).
[7] T. A. LEONARD and R. A. COVER: *J. Appl. Phys.*, **50**, 3241 (1979).
[8] P. D. CARTER, S. M. L. SIM, H. C. BARR and R. G. EVANS: *Phys. Rev. Lett.*, **44**, 1407 (1980).
[9] E. MCGOLDRICK and S. M. L. SIM: *Opt. Commun.*, **39**, 172 (1981).
[10] L. V. POWERS and R. J. SCHROEDER: *Phys. Rev. A*, **29**, 2298 (1984).
[11] V. ABOITES, T. P. HUGHES, E. MCGOLDRICK, S. M. L. SIM, S. J. KARTTUNEN and R. G. EVANS: *Phys. Fluids*, **28**, 2555 (1985).
[12] F. AMIRANOFF, F. BRIAND and C. LABAUNE: *Phys. Fluids*, **30**, 2221 (1987).
[13] H. C. PANT, K. EIDMANN, P. SACHSENMAIER and R. SIGEL: *Opt. Commun.*, **16**, 396 (1976).
[14] R. E. TURNER, D. W. PHILLION, B. F. LASINSKI and E. M. CAMPBELL: *Phys. Fluids*, **27**, 511 (1984).
[15] D. M. VILLENEUVE, H. A. BALDIS and C. J. WALSH: *Phys. Fluids*, **28**, 1454 (1985).
[16] C. LABAUNE, E. FABRE and G. BONNAUD: *J. Plasma Phys.*, **38**, 445 (1987).
[17] P. E. YOUNG, B. F. LASINSKI, W. L. KRUER, E. A. WILLIAMS, K. G. ESTABROOK, E. M. CAMPBELL, R. P. DRAKE and H. A. BALDIS: *Phys. Rev. Lett.*, **61**, 2766 (1988).
[18] E. F. GABL, R. L. BERGER, GAR. E. BUSH, P. M. CAMPBELL, R. J. SCHROEDER, C. L. SHEPARD and J. A. TARVIN: *Phys. Fluids, B*, **1**, 1850 (1989).
[19] J. MEYER, Y. ZHU and F. L. CURZON: *Phys. Fluids B*, **1**, 650 (1989).
[20] A. I. AVROV, V. YU. BYCHENKOV, O. N. KROKHIN, V. V. PUSTOVALOV, A. A. RUPASOV, V. P. SILIN, G. V. SKLIZKOV, V. T. TIKHONCHUK and A. S. SHIKANOV: *Sov. Phys. JETP*, **45**, 507 (1977).
[21] E. Z. GUSAKOV: *Sov. Tech. Phys. Lett.*, 3, 504 (1977).
[22] R. W. SHORT, W. SEKA, K. TANAKA and E. A. WILLIAMS: *Phys. Rev. Lett.*, **52**, 1496 (1984).
[23] B. K. SINHA, S. R. KUMBHARE and G. P. GUPTA: *Phys. Rev. A*, **36**, 4859 (1987).
[24] R. A. LONDON and M. D. ROSEN: *Phys. Fluids*, **29**, 3813 (1986).

[25] C. S. LIU and M. N. ROSENBLUTH: *Phys. Fluids*, **19**, 967 (1976).
[26] A. SIMON, R. W. SHORT, E. A. WILLIAMS and T. DEWANDRE: *Phys. Fluids*, **26**, 3107 (1983).
[27] A. A. ZOZULYA, V. P. SILIN and V. T. TIKHONCHUK: *Sov. J. Plasma Phys.*, **13**, 305 (1987).
[28] D. W. FORSLUND, J. M. KINDEL and E. L. LINDMAN: *Phys. Fluids*, **18**, 1002 (1975).
[29] Z. Z. CHEN and E. SCHIFANO: IFAM Internal Report, Jan. 1988.
[30] N. G. BASOV, YU. A. ZAKHARENKOV, N. N. ZOREV, G. V. SKLIZKOV, A. A. RUPASOV, A. S. SHIKANOV: in *Heating and Compression of Thermonuclear Targets by Laser Beam*, edited by N. G. BASOV (Cambridge University Press, Cambridge 1986), and references therein.
[31] A. GIULIETTI, D. GIULIETTI, D. BATANI, V. BIANCALANA, L. GIZZI, L. NOCERA and E. SCHIFANO: *Phys. Rev. Lett.*, **63**, 524 (1989).